



Sources and mixing behavior of chromophoric dissolved organic matter in the Taiwan Strait



Hui Lin^a, Yihua Cai^{a,*}, Xiuwu Sun^b, Guoxiang Chen^a, Bangqin Huang^a, Hua Cheng^c, Min Chen^a

^a State Key Laboratory of Marine Environmental Science, Xiamen University, Xiamen 361005, China

^b Third Institute of Oceanography, State Oceanic Administration, Xiamen 361005, China

^c Department of Physics, Xiamen University, Xiamen 361005, China

ARTICLE INFO

Article history:

Received 29 March 2015

Received in revised form 15 April 2016

Accepted 8 November 2016

Available online 10 November 2016

Keywords:

Absorption coefficient

Fluorescence

Chromophoric dissolved organic matter

Taiwan Strait

Hydrological control

ABSTRACT

The distribution and dynamics of chromophoric dissolved organic matter (CDOM) in the Taiwan Strait were investigated through an examination of the seasonal and geographic variations of its optical properties. The absorption coefficient a_{280} showed higher values in the onshore area occupied by the low salinity Min-Zhe Coastal Current and river plumes, and decreased toward offshore waters dominated by the South China Sea seawater and Kuroshio Current. The spectral slope over wavelengths of 275–295 nm ($S_{275-295}$) also increased with increasing distance from the coastline. The seasonal variations of a_{280} and $S_{275-295}$ were closely related to the salinity, where high a_{280} and low $S_{275-295}$ were associated with low salinity. Three fluorescent components, including two protein-like and one humic-like, were further identified with the application of parallel factor analysis to excitation–emission matrix spectra. The seasonal variations of fluorescent components were similar to d_{280} , and the marine autochthonous fluorescent component increased from 38 to 44% along with the increasing fraction of South China Sea seawater and the Kuroshio Current in the Taiwan Strait. The spatial and seasonal distribution of bulk CDOM and fluorescent components suggested the important contribution of terrestrial input and the hydrological control of CDOM dynamics in the Taiwan Strait. A mixing model of three end-members, coastal water, river plumes and offshore seawater, was applied to estimate the CDOM removal or addition in the Taiwan Strait. The results revealed moderate addition of bulk CDOM to the Taiwan Strait in summer, likely contributed by the primary production and input from ungauged small coastal rivers. During winter, CDOM was conservatively mixed in the northern Taiwan Strait but showed up to 50% removal in the southern Taiwan Strait.

© 2016 Elsevier B.V. All rights reserved.

1. Introduction

Dissolved organic matter (DOM), one of the largest pools of reduced carbon in the marine environment, is poorly characterized and thus hinders an understanding of its dynamics (Coble, 2007; Yamashita and Jaffe, 2008; Hansell et al., 2009). However, DOM is actively involved in the marine food web as energy and nutrient sources and as byproducts of biological metabolisms (Dyhrman et al., 2006; Jiao et al., 2010; Wetzel and Wheeler, 2007). Because of its binding affinity and photo-reactivity, DOM also regulates the speciation and bioavailability of trace metals such as iron, and serves as an important mediator in numerous photochemical reactions (Barbeau et al., 2001; Bergquist et al., 2007; Hansell and Carlson, 2015). The great reactivity and bioavailability of DOM therefore suggest its potential role in global carbon cycles, which has been the subject of numerous investigations (e.g., Nelson and Siegel, 2013; Nelson et al., 2010). DOM in the open ocean is dominated by autochthonous input (Coble, 2007; Hansell and Carlson, 2015). In contrast, terrestrially-derived DOM composes a substantial fraction of

bulk DOM in marginal seas (Fichot and Benner, 2012; Fichot et al., 2013), and its reactivity and transformation greatly impact the distribution, fate and cycling of organic carbon in marine environments (Hansell and Carlson, 2015; Bianchi et al., 2013).

Chromophoric DOM (CDOM) represents an important fraction of DOM which contributes to the ocean colour by absorbing light over a broad range of UV and visible wavelengths (Coble, 2007). Owing to its intense absorption in the blue range (350–500 nm), CDOM has a critical impact on the light availability, and therefore influences the primary production in aquatic ecosystems (Blough and Del Vecchio, 2002; Del Vecchio and Blough, 2004; Nelson and Siegel, 2013). In coastal areas, distribution and composition of CDOM are generally controlled by physical mixing of terrestrial and autochthonous sources, although removing processes, such as photo-bleaching and microbial degradation are also widely observed (Coble, 2007; Nelson and Siegel, 2013; Nelson et al., 2010; Yamashita et al., 2013). Various optical analytical techniques combined with statistical methods have been developed to analyze the CDOM abundance and composition in the investigation of the effect of hydrological and biogeochemical processes on the quantity and quality of CDOM in dynamic coastal environments (Cai et al., 2013; Guo and Santschi, 2007; Helms et al., 2008; Stedmon et al., 2003; Twardowski et

* Corresponding author.

E-mail address: yihua_cai@xmu.edu.cn (Y. Cai).

al., 2004). For example, the shape of the CDOM absorption spectrum, or spectral slope, is an indicator of the molecular weight (MW) of DOM controlled by source properties and biological alteration (Helms et al., 2008; Twardowski et al., 2004). Thus, the spectral slope has been utilized to trace the terrestrial input, water mixing and the variation of CDOM quality in coastal environments (Cai et al., 2013; Guo et al., 2007). Meanwhile, the three-dimensional excitation-emission matrix (EEM) fluorescence measurements and subsequent parallel factor analysis (PARAFAC), a multivariate data analysis method (Stedmon et al., 2003), have been applied to characterize the individual components contributing to the fluorescent DOM in coastal environments, allowing for the examination of CDOM dynamics and its spatio-temporal distribution when combined with environmental and ecological settings (Coble, 2007; Fellman et al., 2010; Guo et al., 2011; Kowalczyk et al., 2010).

The Taiwan Strait borders Mainland China to the west and Taiwan to the east, and connects two large river-dominated marginal seas in the western Pacific Ocean: the East China Sea (ECS) and South China Sea (SCS) (Fig. 1). It is a shallow strait with an average depth of 60 m, spanning approximately 350 km meridionally and 180 km transmeridionally (Hong et al., 2011a). The Taiwan Strait serves as a crucial channel for water exchange between the western Pacific Ocean and the Chinese marginal seas. The Kuroshio Current and the SCS seawater flow northward along the Penghu Channel between Taiwan and the Penghu Islands and reach the ECS shelf (average 2.28 Sv in winter and 3.32 Sv

in summer) (Hu et al., 2010). However, the Min-Zhe Coastal Current transports a large amount of associated organic matter and nutrients through the Taiwan Strait from the ECS to the SCS during winter along with the water transportation (1.02 Sv) (Jan et al., 2002; Hu et al., 2010; Zhang et al., 2013). In addition, the Taiwan Strait receives the direct discharge of freshwater from coastal rivers, including the Minjiang, Jiulong and Hanjiang Rivers along the western coast and the Tamsui, Zhuoshui, and Tsengwen Rivers along the eastern coast. Furthermore, the Pearl River plume intrudes into the southern part of the Taiwan Strait during summer. Upwelling systems are observed along the western coast and the Minnan-Taiwan Bank in the Taiwan Strait during summer.

Distinct seasonal variations of hydrological conditions exert influences on the biogeochemistry of the Taiwan Strait (Hong et al., 2011a, 2011b; Naik and Chen, 2008). Until now, most of the biogeochemical investigations in the Taiwan Strait focused on the distribution patterns and behavior of nutrients and bulk organic carbon (Chen et al., 2004; Hong et al., 2011a; Wang et al., 2013). CDOM dynamics in the Taiwan Strait are, instead, poorly examined although some researchers have investigated the seasonal variations and mixing behavior of CDOM in the watersheds and estuaries along both sides of the Taiwan Strait (Guo et al., 2007, 2011; Yang et al., 2012, 2013). In our study, seawater samples were collected from the Taiwan Strait during spring, summer and winter 2012 for analysis of the CDOM absorption spectrum and fluorescence in order to understand its biogeochemistry in response to the

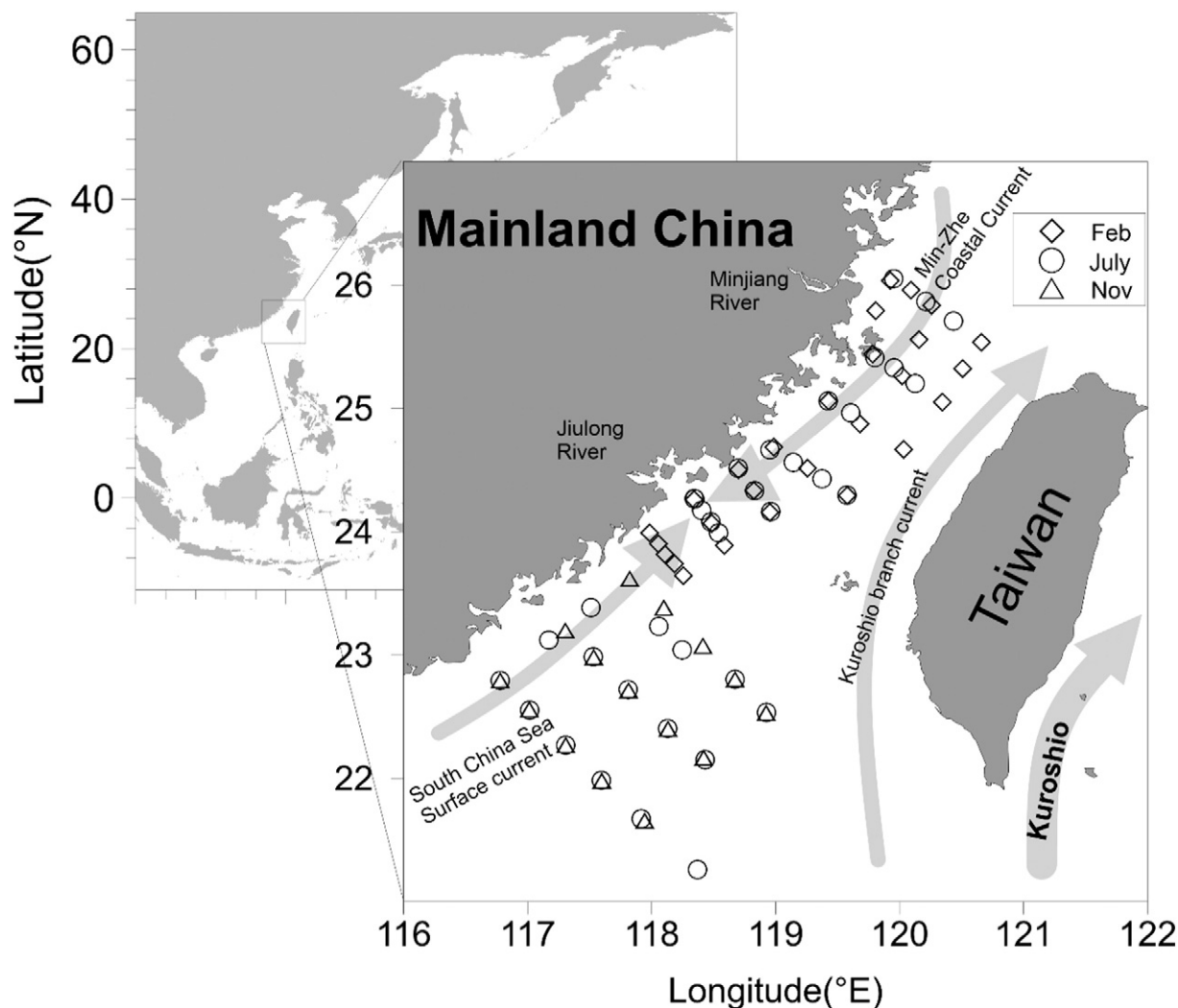


Fig. 1. Map of the Taiwan Strait. Sampling locations are marked by diamonds for February, circles for July and triangles for November 2012.

hydrological regimes and environmental factors in the Taiwan Strait. Three fluorophores were identified with the application of the PARAFAC program. The optical properties were examined against the hydrological parameters and biological activities. A three end-member model was developed to further examine the mixing behavior of CDOM in the Taiwan Strait. The result could be beneficial to understanding the CDOM dynamics in the Taiwan Strait and may shed light on organic carbon cycling in the marginal seas of the western Pacific Ocean.

2. Methods

2.1. Sample collection

Three cruises were conducted in the Taiwan Strait onboard R/V Yanping II from 21st February to 1st March, 1st to 7th July and 20th to 23rd November 2012, representing the spring, summer and winter seasons. Eight cross-strait transects covering the middle-north part of the strait were surveyed in the spring and three transects located at the southern part of the strait in the winter cruises, while the whole strait was surveyed in the summer cruise (Fig. 1).

Seawater samples for CDOM measurement were collected in 12 L Niskin bottles mounted on a rosette sampler with a Seabird CTD. Immediately after sampling, the seawater samples were filtered through pre-combusted (450 °C for 5 h) GF/F filters (Whatman, 0.7 μm pore size). The filtrate was stored in 60 mL pre-combusted (450 °C for 5 h) amber borosilicate glass vials with Teflon-lined caps after triple rinsing. The samples were kept in cold (4 °C) and dark conditions for <1 month until analysis in the laboratory. Previous investigations report that the storage effect on CDOM properties is negligible during one month storage (Stedmon et al., 2000; Walker et al., 2009). An aliquot of the filtrate sample was collected and kept frozen until the analysis of dissolved organic carbon (DOC), when the concentration was measured on a high temperature combustion total organic carbon analyzer (Shimadzu TOC VCPH). The total DOC blank (including Milli-Q water, acid for sample acidification, and the instrument blank) was generally <2 μM. Precision was better than 2% and the accuracy was within 1% based on the analysis of a deep seawater DOC standard (Cai et al., 2008, 2013).

2.2. Absorption measurements

Water samples were warmed overnight to room temperature in the dark and then the CDOM absorption spectra were triply scanned over the wavelength range 240–900 nm in 0.2 nm increments on a Shimadzu UV2500 UV-Vis spectrophotometer with 10 cm path length quartz cuvettes. The blanks were corrected by subtracting the Milli-Q water absorption spectrum while the correction for the refractive index effect was conducted by subtracting the average absorbance between 800 and 900 nm of each sample spectrum. The absorption coefficient (a_λ) was calculated from the absorbance (A_λ) using the equation:

$$a_\lambda = 2.303 \times A_\lambda / l \quad (1)$$

where l is the cuvette length in meters. CDOM concentration was determined by the absorption coefficient at a specific wavelength for which 280 nm was chosen (a_{280}). Strong correlations were found between absorption coefficients at wavelengths of 254, 280 and 350 nm, supporting a_{280} as an indicator of CDOM concentration in the Taiwan Strait.

An exponential regression of a_λ and the spectral slope over a wavelength range of 275–295 nm ($s_{275-295}$) was applied to describe the exponential decrease of absorbance with increasing wavelength:

$$a_\lambda = a_{\lambda_0} e^{-s_{275-295}(\lambda-\lambda_0)} \quad (2)$$

where a_{λ_0} is the absorbance at the reference wavelength of 280 nm (λ_0). Spectral slope parameters are widely used as an excellent indicator of the sources, MW and diagenetic status of CDOM in aquatic

environments, and $s_{275-295}$ is demonstrated to be a reliable proxy of CDOM average MW and a potential indicator of DOM photo-bleaching intensity in the marine environment (Helms et al., 2008). It is also proposed as a tracer of terrigenous DOC in fluvial-influenced coastal margins (Fichot and Benner, 2012).

2.3. Fluorescence EEM analyses and PARAFAC modeling

Fluorescence of the water samples was measured using a Cary Eclipse Spectrofluorometer (Varian, Australia) equipped with a 15 W Xeon pulse lamp as the excitation light source and a ×2 photomultiplier tube as the emission detector. EEMs were generated over an excitation wavelength range from 200 to 450 nm at 5 nm intervals and an emission wavelength range from 230 to 600 nm at 2 nm intervals. In order to correct Rayleigh and Raman scatter peaks, the Milli-Q water blank values were subtracted from each sample EEM. A dilution series of known concentration of quinine sulfate was used to normalize the fluorescence intensity, which was then converted to quinine sulfate unit (QSU) equivalents.

PARAFAC was used to resolve all EEM spectra. The “N-way tool box” on the MatLab software platform (Version 7.8.0.347, R2009a) was used to decompose EEMs into individual fluorescent components (Stedmon and Bro, 2008). Split-half validation and residual analysis were carried out to validate the three component model generated by PARAFAC.

2.4. Three end-member mixing model

In order to determine the fraction of CDOM deviating from conservative mixing owing to biological production and physiochemical processing, an algebraic three end-member mixing model is developed to describe the CDOM dynamics in the Taiwan Strait (Rosón et al., 1997), which is a hydrologically dynamic region as revealed by previous studies (Hong et al., 2011a, 2011b; Wu et al., 2007). Three typical water masses are selected as end-members based on their distinct hydrological characterization (Fig. 2). The dilution water (DW) represents the Min-Zhe Coastal Current in the winter and river plumes in the summer, and is characterized by low salinity as a result of dilution by fresh water. The SCS surface water (SCSSW) and the subsurface water (SCSubW), which is 150–200 m deeper than the SCSSW, have high salinity. The po-

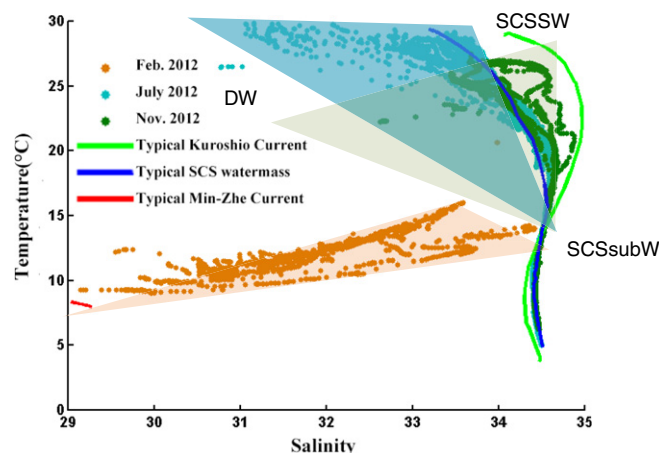


Fig. 2. Diagram of potential temperature versus salinity in spring (orange dots), summer (light blue dots) and winter (dark green dots) in the Taiwan Strait. Three typical seawater masses, including the Min-Zhe Coastal Current water (red line) collected in the southern part of East China Sea, Kuroshio Current water collected east of the Luzon Strait (green line) and South China Sea water collected near the SEATS station (blue line) are plotted together. Data for the three typical currents were downloaded from http://www.nodc.noaa.gov/OC5/WOD09/pr_wod09.html.

tential temperature (θ) and salinity (S) of the water samples are used to calculate the fractions of each water source:

$$\begin{cases} \theta_{DW}f_{DW} + \theta_{SCSSubW}f_{SCSSubW} + \theta_{SCSSW}f_{SCSSW} = \theta \\ S_{DW}f_{DW} + S_{SCSSubW}f_{SCSSubW} + S_{SCSSW}f_{SCSSW} = S \\ f_{DW} + f_{SCSSubW} + f_{SCSSW} = 1 \end{cases} \quad (3)$$

where f_{DW} , $f_{SCSSubW}$, f_{SCSSW} are the fractions of DW, SCSSubW and SCSSW; and θ_{DW} , $\theta_{SCSSubW}$, θ_{SCSSW} and S_{DW} , $S_{SCSSubW}$, S_{SCSSW} are the potential temperature and salinity of the three end-members. Table 1 displays two different seasonal sets of average and standard deviation of all parameters involved in the model, including potential temperature, salinity, a_{280} , DOC, and the three fluorescent components.

a_{280} was selected to represent the bulk CDOM concentration. With the fraction of each water source derived from Eq. (3), the conservative absorption coefficient a_{280}° was predicted following the three end-member mixing equation:

$$a_{280}^{\circ} = a_{280_{DW}}f_{DW} + a_{280_{SCSSubW}}f_{SCSSubW} + a_{280_{SCSSW}}f_{SCSSW} \quad (4)$$

where $a_{280_{DW}}$, $a_{280_{SCSSubW}}$, $a_{280_{SCSSW}}$ are the a_{280} values of the three water mass end-members. The differences between the modelled conservative values and the measured values a_{280} (in situ), denoted as Δa_{280} , are estimated using the following equation:

$$\Delta a_{280} = a_{280}(\text{in situ}) - a_{280}^{\circ} \quad (5)$$

The positive Δa_{280} indicated the CDOM addition beyond the conservative mixing. On the contrary, the negative Δa_{280} values were associated with CDOM removal. In addition, DOC and three fluorescent

components derived from the PARAFAC program were analyzed using the same model, generating ΔDOC , ΔC1 , ΔC2 and ΔC3 . The model uncertainty for each parameter generally arises from the designated range of potential temperature, salinity and parameter for each end-member. Since the potential temperature and salinity of each end-member are well defined with a small variation, the uncertainty of every parameter is largely derived from its own variation. Table 2 displays the field measurement, model output and uncertainty of each parameter in two different seasons.

3. Results

3.1. Water masses

Based on the spatial distribution of hydrological properties (salinity and temperature) during sampling cruises, the water masses in the Taiwan Strait are well characterized in previous studies (Hu et al., 2010; Naik and Chen, 2008). In our study, the high temperature and high salinity water derived from the SCS waters and Kuroshio Current was present in the eastern Taiwan Strait all year round. However, the water masses in the western Taiwan Strait showed significant seasonal variation. During spring, the low temperature and low salinity Min-Zhe Coastal Current spread southward along the western coast (Fig. 3a and b); and it dissipated in the Taiwan Strait during summer, while several fresh water plumes with high temperature and low salinity were present, being the Minjiang River, Jiulong River and Pearl River plumes from north to south along the west coast (Fig. 3c and d). Several patches of upwelling water with low temperature and high salinity were also defined along the west coast and Minnan-Taiwan Bank in the Taiwan

Table 1
Summary of end-member values applied in the three end-member mixing model. SCSSW, SCSSubW and DW refer to the South China Sea Surface Water, South China Sea Subsurface Water and Dilution Water. DW includes the Min-Zhe Coastal Current during spring and winter, and river plume waters during summer.

| Season | End-member parameters | Water masses | | |
|--------|-------------------------------|----------------|----------------|----------------|
| | | SCSSW | SCSSubW | DW |
| Summer | Potential temperature [°C] | 28.048 ± 0.475 | 16.301 ± 0.445 | 28.805 ± 0.651 |
| | Salinity | 33.641 ± 0.048 | 34.585 ± 0.009 | 24.500 ± 0.085 |
| | a_{280} [m^{-1}] | 0.446 ± 0.196 | 0.477 ± 0.032 | 1.345 ± 0.091 |
| | C1 [QSU] | 1.524 ± 0.456 | 1.528 ± 0.325 | 4.889 ± 2.745 |
| | C2 [QSU] | 0.710 ± 0.411 | 0.822 ± 0.143 | 1.381 ± 0.057 |
| | C3 [QSU] | 5.227 ± 0.944 | 1.967 ± 0.501 | 4.268 ± 2.170 |
| Winter | Potential temperature [°C] | 26.903 ± 0.156 | 17.300 ± 0.723 | 22.279 ± 0.029 |
| | Salinity | 33.641 ± 0.048 | 34.585 ± 0.009 | 24.500 ± 0.085 |
| | a_{280} [m^{-1}] | 0.453 ± 0.048 | 0.479 ± 0.027 | 1.455 ± 0.057 |
| | C1 [QSU] | 0.789 ± 0.239 | 1.641 ± 0.461 | 5.527 ± 0.292 |
| | C2 [QSU] | 0.319 ± 0.026 | 0.768 ± 0.149 | 2.407 ± 0.403 |
| | C3 [QSU] | 1.624 ± 0.588 | 3.081 ± 1.244 | 7.019 ± 1.021 |

Table 2
Summary of field concentration and model outcome of a_{280} , DOC and three fluorescence components and their differences between field observation and model estimation and model uncertainty. Owing to the conservative trends in the northern Taiwan Strait during winter, only the southern part of the Taiwan Strait was taken into account to estimate the removal percentage.

| Season | Statistic Parameter | a_{280} [m^{-1}] | C1 [QSU] | C2 [QSU] | C3 [QSU] |
|-------------------------------------|-------------------------------------|-------------------------------|----------------|----------------|----------------|
| Summer | In situ value (\bar{x}) | 0.711 ± 0.347 | 2.832 ± 2.814 | 1.022 ± 0.613 | 3.136 ± 2.315 |
| | Model outcome (\bar{x}°) | 0.617 ± 0.193 | 2.352 ± 1.127 | 1.075 ± 0.412 | 2.969 ± 1.042 |
| | Difference (Δx) | 0.094 ± 0.36 | 0.348 ± 2.604 | -0.061 ± 0.571 | -0.031 ± 2.351 |
| | Uncertainty (ϵ_x) | 0.148 | 0.182 | 0.100 | 0.097 |
| | Addition or removal percentage (%) | 13.2 ± 1.9 | 12.9 ± 2.3 | -3.1 ± 0.3 | -1.0 ± 0.1 |
| | Winter | In situ value (\bar{x}) | 0.715 ± 0.346 | 1.931 ± 1.589 | 0.931 ± 0.658 |
| Model outcome (\bar{x}°) | | 0.857 ± 0.218 | 2.709 ± 0.885 | 1.175 ± 0.383 | 3.872 ± 0.962 |
| Difference (Δx) | | -0.279 ± 0.240 | -0.872 ± 1.413 | -0.289 ± 0.676 | -1.364 ± 1.593 |
| Uncertainty (ϵ_x) | | 0.0475 | 0.113 | 0.018 | 0.067 |
| Addition or removal percentage (%) | | -49.3 ± 2.3 | -47.5 ± 5.4 | -32.6 ± 0.6 | -54.4 ± 3.6 |

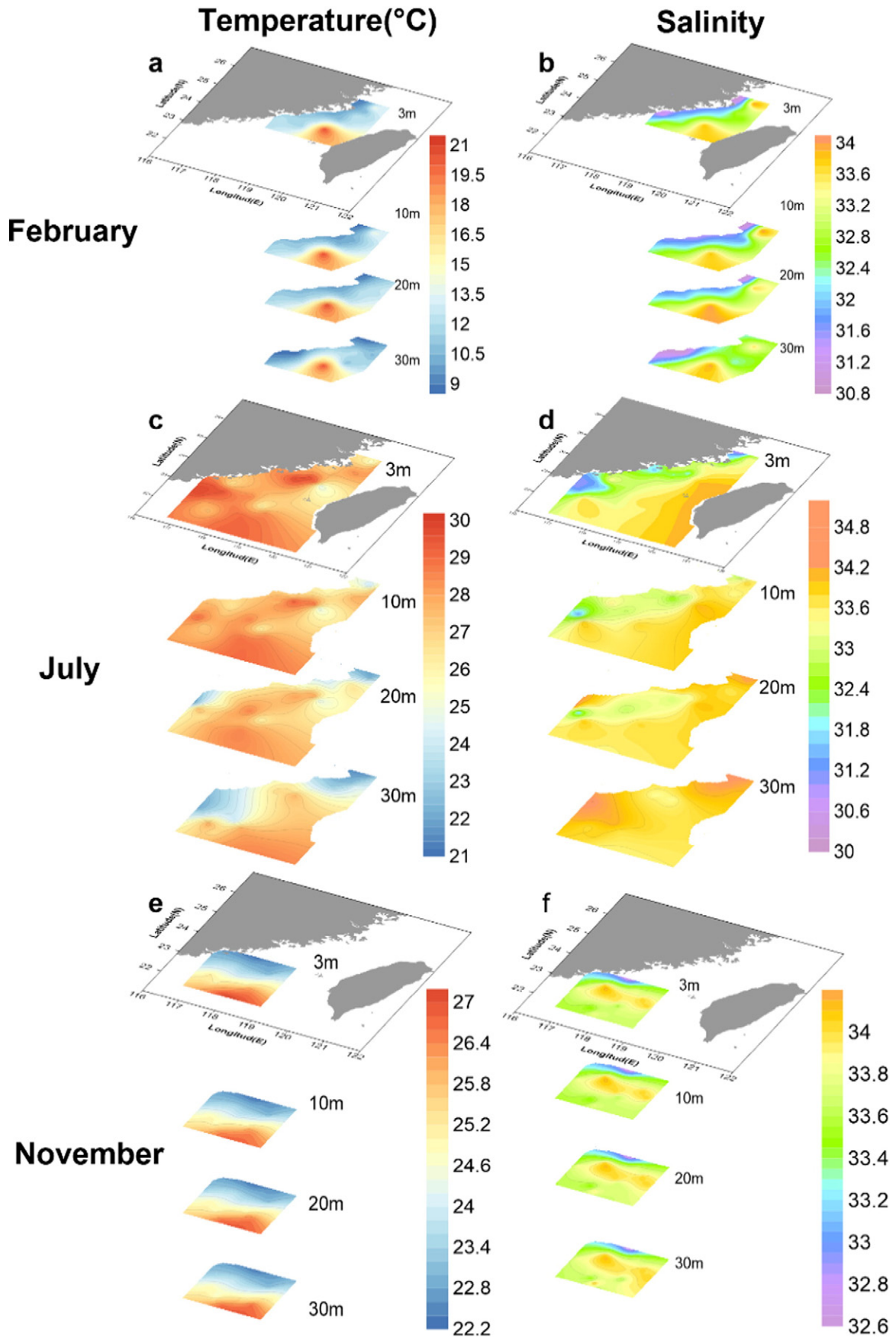


Fig. 3. Spatial distribution of (left) temperature (°C) and (right) salinity in the western Taiwan Strait in 2012.

Strait which were induced by the northward movement of the SCS waters and Kuroshio Branch Current, and subsequent uplift owing to the topographical conditions (Fig. 3c and d). Although hydrological data were only collected in the southern part of the Taiwan Strait during the 2012 winter, the peripheral signal of the Min-Zhe Coastal Current was observed in the northwest part of the surveyed area (Fig. 3e and f). The T-S diagram, which was plotted from all the hydrological data collected during all three cruises, suggested that the seawater in the Taiwan Strait was apparently derived from the SCS waters, the Kuroshio Current, riverine freshwater input and the Min-Zhe Coastal Current, although seasonal variations of the contribution of each water mass were significant (Fig. 2).

3.2. Absorption coefficient, spectral slope coefficient and DOC

The absorption coefficient a_{280} varied from 0.06 to 2.46 m^{-1} in the Taiwan Strait during all three cruises. It showed a higher value in the coastal regions which were occupied by the Min-Zhe Coastal Current during spring and winter, and by the river plume waters during summer. Du et al. (2010) report high a_{412} value in the two major western coastal estuaries, which was consistent with our a_{280} results. The a_{280} value decreased in offshore waters which were dominated by the SCS waters and Kuroshio Current (Fig. 4).

Vertically, surface water usually had a higher a_{280} value than deep water with higher salinity, although a subsurface maximum could be

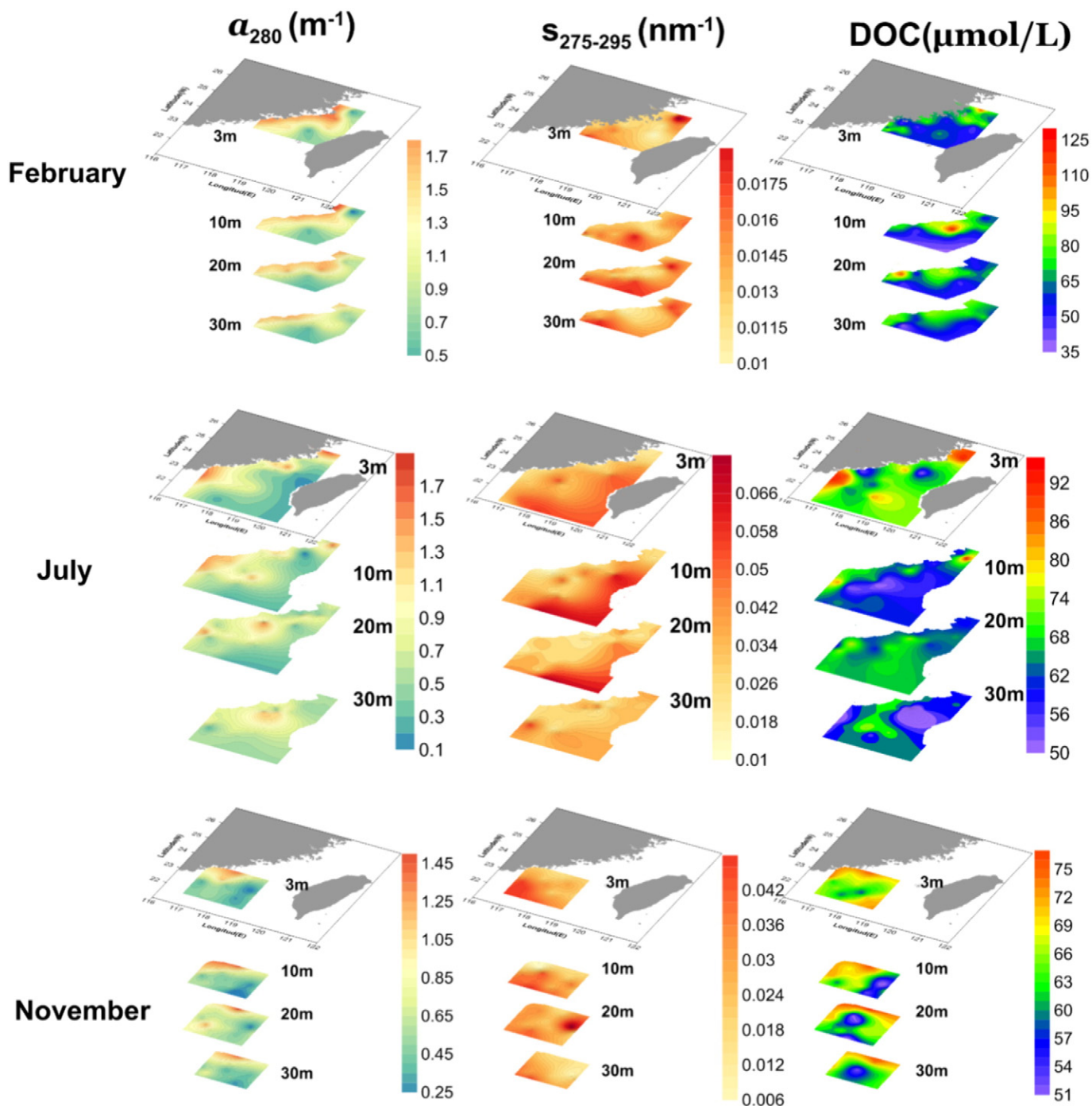


Fig. 4. Spatial distribution of (left) a_{280} (m^{-1}), (middle) $S_{275-295}$ (m^{-1}) and (right) DOC ($\mu\text{mol}\cdot\text{L}^{-1}$) from 3 m to 30 m in (top) spring, (middle) summer and (bottom) winter, 2012, in the Taiwan Strait.

observed in some SCS water dominant areas during summer (Figs. 4, S1–6), likely due to the photo-degradation of DOM in the surface water and/or autochthonous production of DOM associated with the subsurface chlorophyll *a* maximum (Hong et al., 2011b; Jørgensen et al., 2011). This was consistent with the biological activities in the euphotic zone contributing the high autochthonous CDOM. The relatively higher terrestrial input in the surface water brought by the river plumes and Min-Zhe coastal current with lower salinity also enhanced the surface CDOM concentration.

The a_{280} value also showed significant seasonal variation, with average values of 1.23 ± 0.32 , 0.71 ± 0.35 and $0.58 \pm 0.33 \text{ m}^{-1}$ in spring, summer and winter (Fig. 5). Significant inverse linear correlations existed between the salinity and a_{280} in all three cruises ($p < 0.01$), implying the major terrestrial contribution to the CDOM pool in the Taiwan Strait and a possible dilution through a physical mixing with seawater. However, the data points scattered over the mixing line in summer and winter, which implied additional biogeochemical processes, including microbial deposition and photo-degradation, beyond the simple two end-member mixing responsible for non-conservative behavior, especially in the southern part of the Taiwan Strait. Further discussion about conservative and non-conservative mixing dynamics in the Taiwan Strait is presented in the next section.

The slope coefficient between 275 and 295 nm ($S_{275-295}$) varied between 0.0014 and 0.0806 nm^{-1} . As expected, the spectral slope was flatter in the coastal area and steeper in the offshore, which indicated that high MW (HMW) CDOM derived from fluvial input prevails in the coastal area, but marine-derived low MW (LMW) CDOM in the offshore water (Fichot and Benner, 2012; Helms et al., 2008). Vertically,

$S_{275-295}$ generally increased from the surface to bottom water in the northern and central Taiwan Strait, but no consistent vertical pattern was shown in the southern Taiwan Strait (Fig. 4, S1–S6). $S_{275-295}$ also varied seasonally: 0.0144 ± 0.0022 , 0.0310 ± 0.090 , and $0.0288 \pm 0.0123 \text{ nm}^{-1}$ in spring, summer and winter. Positive linear relationships between slope and salinity were significant in spring ($R^2 = 0.478$, $p < 0.01$), but not in summer and winter ($p > 0.01$) (Fig. 5). This supported the observed scattering of a_{280} data in the southern part of the Taiwan Strait and indicated that the non-conservative mixing of fluvial input and marine dominant CDOM during summer and winter is accompanied by an alteration of the MW and quality of the DOM (Helms et al., 2008).

During all three cruises, DOC ranged from 35.3 to $123.0 \mu\text{mol/L}$ in the Taiwan Strait. Similar to the vertical distribution of a_{280} , DOC was usually prominent in the surface layer and decreased with depth (Fig. 5 S1–S6). The vertical distribution pattern of DOC in the Taiwan Strait is also similar to that in the SCS but significantly higher at the surface (Dai et al., 2009). No obvious seasonal variation of DOC concentration was observed: 67.1 ± 14.9 , 65.4 ± 11.5 and $62.6 \pm 9.2 \mu\text{mol/L}$ in spring, summer and winter. Unlike a_{280} , which had a conservative trend with salinity in spring, DOC had a vague relationship with salinity in spring ($R^2 = 0.18$, $p > 0.05$), likely due to the mixing of non-chromophorous DOC in the bulk DOM pool (Fig. 5). However, in summer and winter, DOC showed a significant but weak linear inverse correlation with salinity ($p < 0.01$), suggesting the mixing of terrestrial input and marine-dominant DOC (Fig. 5). Nevertheless, the variation of DOC concentration in the high salinity zone was distinguishable. This was consistent with the spatial distribution of CDOM concentration and the spectral slope,

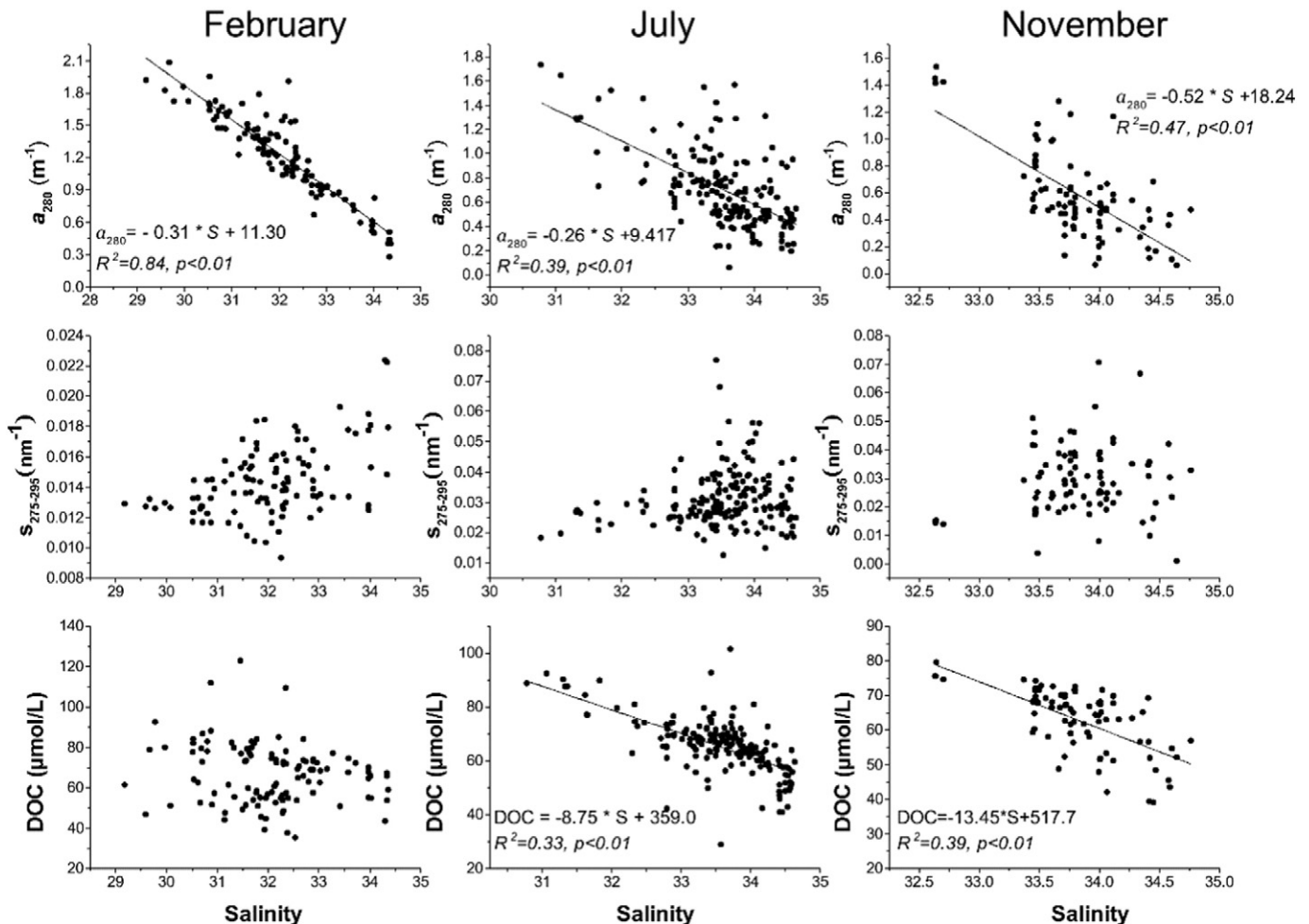


Fig. 5. Salinity versus a_{280} , $S_{275-295}$ and DOC (from top to bottom) in (left) spring, (middle) summer and (right) winter, 2012, in the Taiwan Strait.

and further indicated the multiple DOC sources in the southern part of the Taiwan Strait. These DOC sources may have included the fresher DOC with higher concentration and larger MW in the SCSSW and Kuroshio Current and the aged DOC with LMW at about 40 $\mu\text{mol/L}$ in the SCS deep water (Dai et al., 2009; Lin, 2013). In addition, the biological and physiochemical processes, which caused the non-conservative behavior of CDOM, could have affected the quality and biogeochemical cycling of bulk DOM.

3.3. Fluorescent components

All fluorescence EEMs from the three cruises were sorted and analyzed using the PARAFAC program, and three fluorescent components were revealed (Table 3; Fig. 6). All three components had two excitation maxima and one emission maximum. Component 1 (C1) had a primary excitation maximum peak at 230 nm and a secondary peak at 315 nm with one common emission maximum at 350 nm. The primary peak was analogous to peak N or a combination of peak N and a tryptophan-like component (Guo et al., 2011; Stedmon et al., 2003; Yamashita and Jaffe, 2008). The secondary peak was expected to be the M peak (Coble, 2007). Component 2 (C2) had a broad excitation peak from 250 to 355 nm with an emission wavelength maximum at 435 nm. It was identified as a mix of peaks A and C, which were humic-like components derived from terrestrial input (Guo et al., 2011; Stedmon et al., 2003; Yamashita and Jaffe, 2008). Du et al. (2010) also separately detect peaks A and C in the nearshore waters along the west coast of the Taiwan Strait. Component 3 (C3) had excitation maxima at 225 nm and 275 nm and an emission maximum at 340 nm. The secondary peak resembled the spectral characteristic of tryptophan, which is peak T linked with primary production in previous studies (Coble, 2007; Stedmon and Markager, 2005). All three components had similar variation characteristics with a_{280} . Components were also strongly correlated with each other (data not shown).

Fluorescent DOM intensity and its spatial distribution showed distinct seasonal variations. The bulk fluorescence in spring was almost two-fold those in summer and winter, while the fluorescence in summer was slightly higher than winter. C1 was the predominant fluorescent component in spring with the highest fluorescent intensity (8.2 ± 5.5 QSU). In summer, the fluorescence of C1 dropped to 3.0 ± 3.6 and in winter to 2.1 ± 1.9 QSU, and was comparable to C3 (3.1 ± 2.3 and 2.5 ± 1.5 QSU in July and November). C2 was the minor fluorescent component during all three seasons. Its intensity decreased from 2.8 ± 1.4 in February to 1.0 ± 0.6 and 1.0 ± 0.7 QSU in July and November. Analogous to a_{280} , all fluorescent components showed robust linear correlation with the salinity in spring (Fig. 7). This inverse linearity between fluorescence and salinity was not present in the other two seasons. Simultaneously with the weak correlation between a_{280} and salinity during summer and winter, this might imply that CDOM was subjected to extensive biogeochemical alteration, in which the fluorescence was an indicator more sensitive than absorption.

In the northern and central Taiwan Strait, higher concentrations of fluorescent DOM were shown in the coastal water but the intensity decreased offshore (Figs. 8, S1–S4). Meanwhile, the maximum concentration of fluorescent DOM was observed in outer shelf stations along the southern Taiwan Strait transects (Figs. 8, S5 and S6). Overall, vertical profiles of the three fluorescent components showed a consistent pattern with higher but fluctuating intensity in the surface, and decreasing

intensity with increasing depth (Figs. 8, S1–S6). Similar to a_{280} , subsurface maximum fluorescent components were sometimes observed in the southern Taiwan Strait (Figs. 8, S5 and S6), suggesting the surface microbial decomposition and photo-degradation of labile organic components and/or subsurface autochthonous contribution (Hong et al., 2011b; Jørgensen et al., 2011). The higher fluorescent intensity in the surface water than in the deep water in the Taiwan Strait (which is consistent with its lower salinity) might reflect the terrestrial contribution to the individual fluorescent component and the CDOM pool (Hong et al., 2011b). Meanwhile, biomass growth in the surface water stimulated by the riverine nutrient input would further enhance the production of autochthonous fluorescent components in the Taiwan Strait (Hong et al., 2011a; Yan et al., 2012).

4. Discussion

4.1. Sources and composition of CDOM

C1 resembled peak N, which is proposed as a protein-like component (Coble, 2007). Nonetheless, some investigators also suggest peak N as a PAH component (Murphy et al., 2006) or humic-like substance (Cory and McKnight, 2005; Fellman et al., 2010). Studies conducted in the human-impacted Jiulong River watershed and estuary adjacent to the western Taiwan Strait exclude the possibility of either PAHs or humic substances and, instead, infer that it is a freshwater contributed protein-like material (Guo et al., 2011). Considering the resembling environmental settings in the west coast of the Taiwan Strait, it was reasonable to assume that C1 was riverine protein material.

The C1 fluorescence in spring was greater than that in both summer and winter. Meanwhile, C1 was more abundant in the northern than the southern Taiwan Strait with a decreasing trend from the coastal area to offshore (Fig. 8). This was consistent with the winter and spring southward spreading of the Min-Zhe Coastal Water which entrains large amounts of freshwater to the west coast of the Taiwan Strait and results in the lower salinity there (Hu et al., 2010). Rivers which contribute large amounts of freshwater to the Min-Zhe Coastal Water, including the Yangtze and Minjiang Rivers, are significant sources of terrestrial DOM to the ECS and its adjacent areas (Guo et al., 2014; Li et al., 2007; Xue et al., 2009). During summer, river plumes formed by the freshwater discharge of the Pearl, Jiulong and Minjiang Rivers were clearly observed in the Taiwan Strait (Fig. 3). These river plumes act as large point sources of riverine DOM and therefore enhance the CDOM level in the Taiwan Strait (Guo et al., 2011; He et al., 2010; Yang et al., 2012). The SCS seawater and Kuroshio Branch Current were prevailing in the southern Taiwan Strait in November and the Min-Zhe Coastal Current could reach only the northwest periphery of the investigation area (Fig. 3). In accordance with such a hydrological condition, the riverine input of C1 was minimized in the southern Taiwan Strait although the intensity of C1 was still gently increased in the Min-Zhe Coastal Current influenced area (Fig. 8).

The hydrological settings not only determined the spatio-temporal variation of the riverine protein-like C1 component, but also that of the terrestrially-derived humic-like C2 component. As shown in Fig. 8, high fluorescence intensity of C2 appeared in the coastal regions, strongly affected by the Min-Zhe Coastal current and river plumes, and decreased offshore in the SCS waters and the Kuroshio Current dominated area. The seasonal variation of C2 in the Taiwan Strait also

Table 3
PARAFAC results and characterizations of three fluorescence components in the Taiwan Strait.

| Fluorescence components | Excitation [nm] | Emission [nm] | Fluorophores type | February [QSU] | July [QSU] | November [QSU] |
|-------------------------|-----------------|---------------|--------------------------------|----------------|---------------|----------------|
| Component 1 | 230(315) | 350 | Protein-like (Tryptophan-like) | 8.2 ± 5.5 | 3.0 ± 3.6 | 2.1 ± 1.9 |
| Component 2 | 250–355 | 435 | Humic-like | 2.8 ± 1.4 | 1.0 ± 0.6 | 1.0 ± 0.7 |
| Component 3 | 225(275) | 340 | Protein-like (Tryptophan-like) | 4.9 ± 2.9 | 3.1 ± 2.3 | 2.5 ± 1.5 |

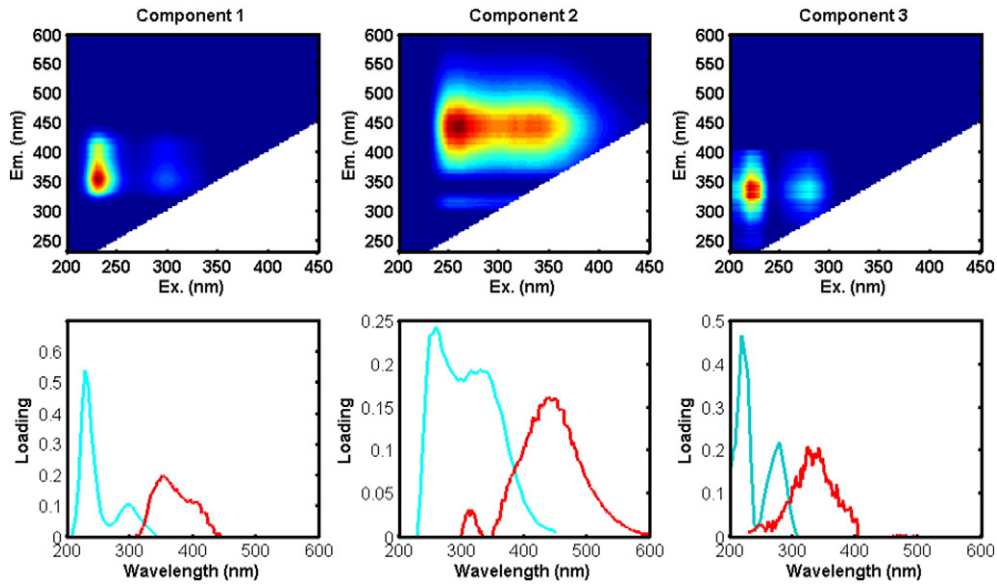


Fig. 6. EEMs of the three divided components (top) and their excitation (light blue) and emission (red) loadings (bottom).

mimicked C1, with higher concentration in February, followed by July and November. The gradually decreasing C2 concentration with increasing depth for all seasons, which was similar to the salinity vertical structure, further implied hydrological control of the spatio-temporal distribution of C2 in the Taiwan Strait.

C3 was likely a protein-like fluorescent component derived from recent primary production (Stedmon and Markager, 2005). The maximum intensity of C3 usually appeared in surface water although it was also shown in mixed-layer water in some stations (10–30 m;

Fig. 8). The subsurface maximum is likely associated with the subsurface chlorophyll *a* maximum (Hong et al., 2011b). Meanwhile, a patch with enhanced C3 concentration existed in the upwelling system located at the Minnan-Taiwan Bank during summer (Fig. 8), which was not observed for C1 and C2. Seasonal monsoon-induced upwelling and year round topographically-derived upwelling pump the nutrient-rich SCS deep water to the subsurface of the Minnan-Taiwan Bank and induce high biomass or even algal blooms (Hong et al., 2011a). Therefore, the highest intensity of C3 associated with the chlorophyll *a* maximum

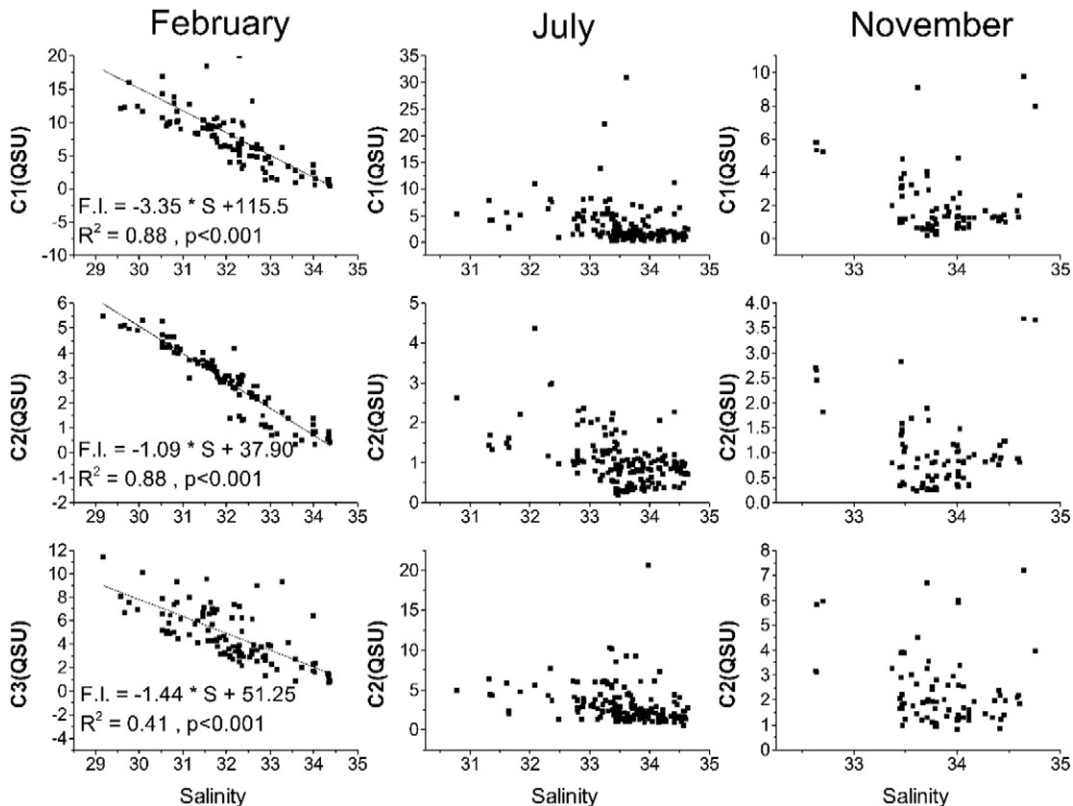


Fig. 7. Salinity versus fluorescent Components 1 (left), 2 (middle) and 3 (right) in spring (top), summer (middle) and winter (bottom), 2012, in the Taiwan Strait.

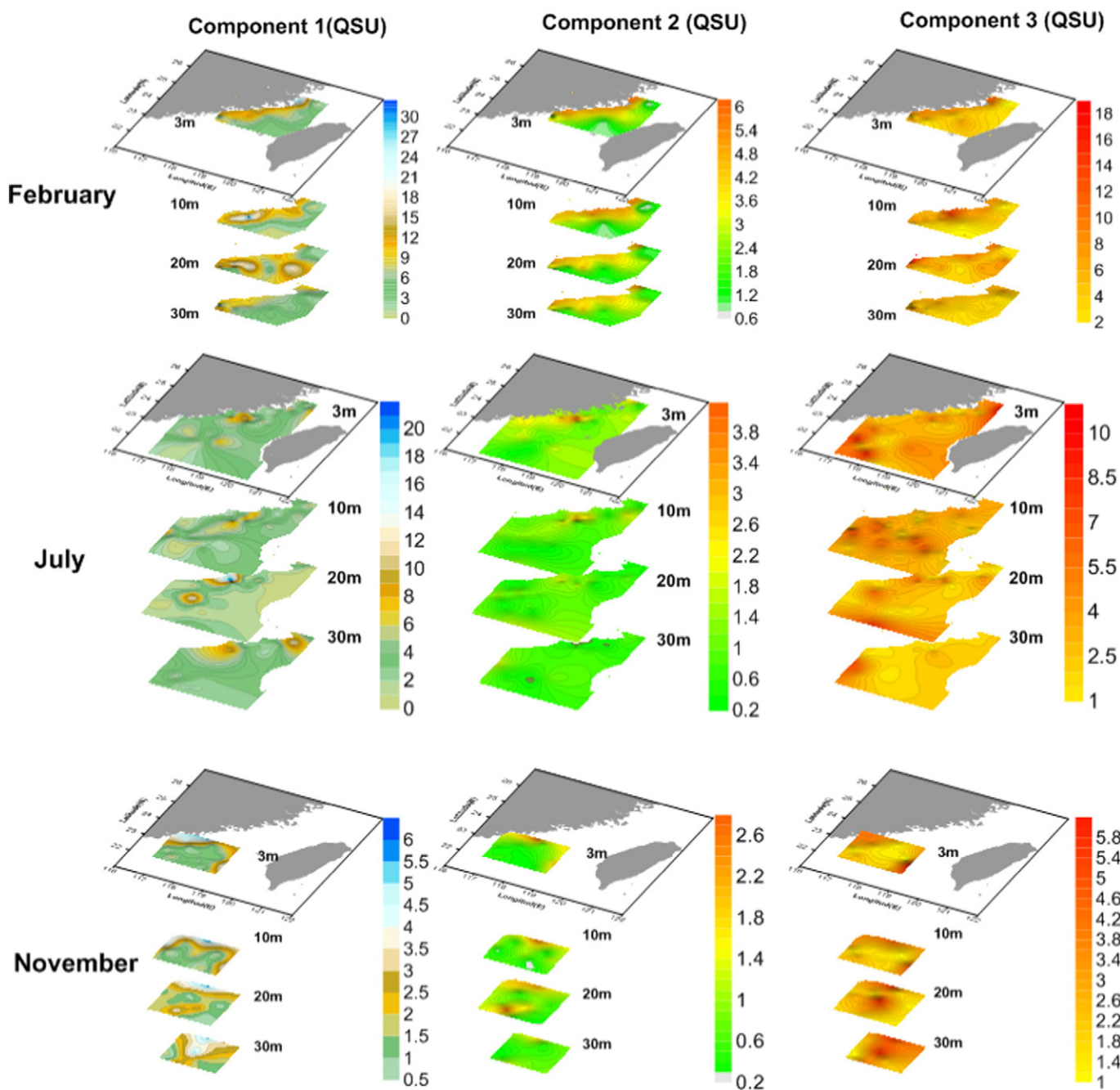


Fig. 8. Spatial distribution of (left) Components 1, (middle) 2 and (right) 3 from 3 to 30 m in (top) spring, (middle) summer and (bottom) winter, 2012, in the Taiwan Strait.

layer and the high primary production demonstrated its autochthonous source from in situ biomass growth. An elevated C3 concentration was also observed in the western coastal Taiwan Strait influenced by the Min-Zhe Coastal Current in February and November and in river plumes in July. However, the observation was more likely to have been caused by biomass growth stimulated by nutrient discharged by these onshore water masses, instead of simple physical mixing. Previous investigation suggests that the Min-Zhe Coastal Current is a major nutrient source supporting the winter primary production of the northern SCS (Han et al., 2013). The Taiwan Strait, as the sole pathway for the intrusion of the Min-Zhe Coastal Current into the northern SCS, undoubtedly presented more significant fractions of autochthonous production of organic matter stimulated by nutrients in the Min-Zhe Coastal Current than the northern SCS.

Based on the average intensity of these components in the three cruises (Table 3), terrestrial input (C1 + C2) comprised 55–69% of total fluorescent DOM, leaving 31–45% as marine autochthonous input. The dominance of terrestrial input in the fluorescent DOM pool in the Taiwan Strait was consistent with the fact that the Taiwan Strait receives large amounts of freshwater discharge from the Yangtze, Pearl and Jiulong Rivers and some other small coastal rivers (Li et al., 2007; Wang et al., 2013). Although the southern and northern parts of the Taiwan Strait were separately sampled in the February and November cruises, both cruises were considered to be conducted under the prevailing northeast monsoon, and these two datasets were therefore combined for comparison with the July dataset. This revealed that the marine autochthonous fluorescent DOM increased from 38 to 44% when the winter northeastern monsoon switched to the summer

southwestern monsoon, consistent with increasing northward transportation of the SCS water through the Taiwan Strait (Liu et al., 2002).

The absorption coefficient a_{280} could be an integrated parameter representing CDOM concentration from both terrestrial and marine sources, which might also include a fraction of fluorescent DOM. The spatial distribution of a_{280} closely resembled fluorescent components C1 and C2 (Figs. 4 and 8) with significant correlation between them (data not shown). Apparently, total CDOM concentration and its spatio-temporal variations were also greatly influenced by the hydrological conditions in the Taiwan Strait as shown by the riverine and terrigenous fluorescent DOM. The robustly inverse correlation between a_{280} and salinity for each cruise also suggested the focal role of the terrestrial input of organic matter and nutrients in determining the CDOM level in the Taiwan Strait through water mass transport and mixing (Fig. 5). Generally, CDOM can be applied as a distinctive indicator to trace the water masses and their seasonal retreat from, and intrusion into, the Taiwan Strait. However, the variable $s_{275-295}$, which did not show a significant correlation with salinity, implied that the CDOM dynamics in the Taiwan Strait might be more complicated than simple physical mixing (Fig. 5).

4.2. CDOM mixing behavior

Since the cruises conducted in February and November were under similar northeast monsoon and hydrological circumstances, these two

datasets were combined to generate a full spring-and-winter dataset covering the Taiwan Strait for comparison with the summer southwest monsoon scenario. A three end-member model was subsequently conducted to resolve the mixing behavior of CDOM in the Taiwan Strait and its geographic and seasonal variations.

4.2.1. Spatial variations

A contrasting CDOM mixing behavior was shown between the northern and southern Taiwan Strait during spring and winter (Fig. 9a and c). Along the salinity gradient, a significant conservative mixing was observed in the northern Taiwan Strait (Fig. 9a), while an apparent removal was revealed in the southern Taiwan Strait (Fig. 9c). In the northern Taiwan Strait, the model indicated that the conservative mixing behavior of CDOM and its fluorescent components was consistent with the field observation of significant inverse correlation between each CDOM parameter with salinity during winter (Figs. 5 and 7). Therefore, physical mixing among the Min-Zhe coastal current and SCS waters was the dominant factor determining the distribution and dynamics of CDOM in the northern Taiwan Strait during winter. In contrast, an effective removal of CDOM and all fluorescent components was indicated by the three end-member mixing model in the southern Taiwan Strait during winter with nearly 50% removal of CDOM and 30–55% removal of fluorescent components during the physical mixing process (Fig. 9b and d; Table 2). Compared to the northern Taiwan Strait, the southern Taiwan Strait had higher $s_{275-295}$ but lower CDOM,

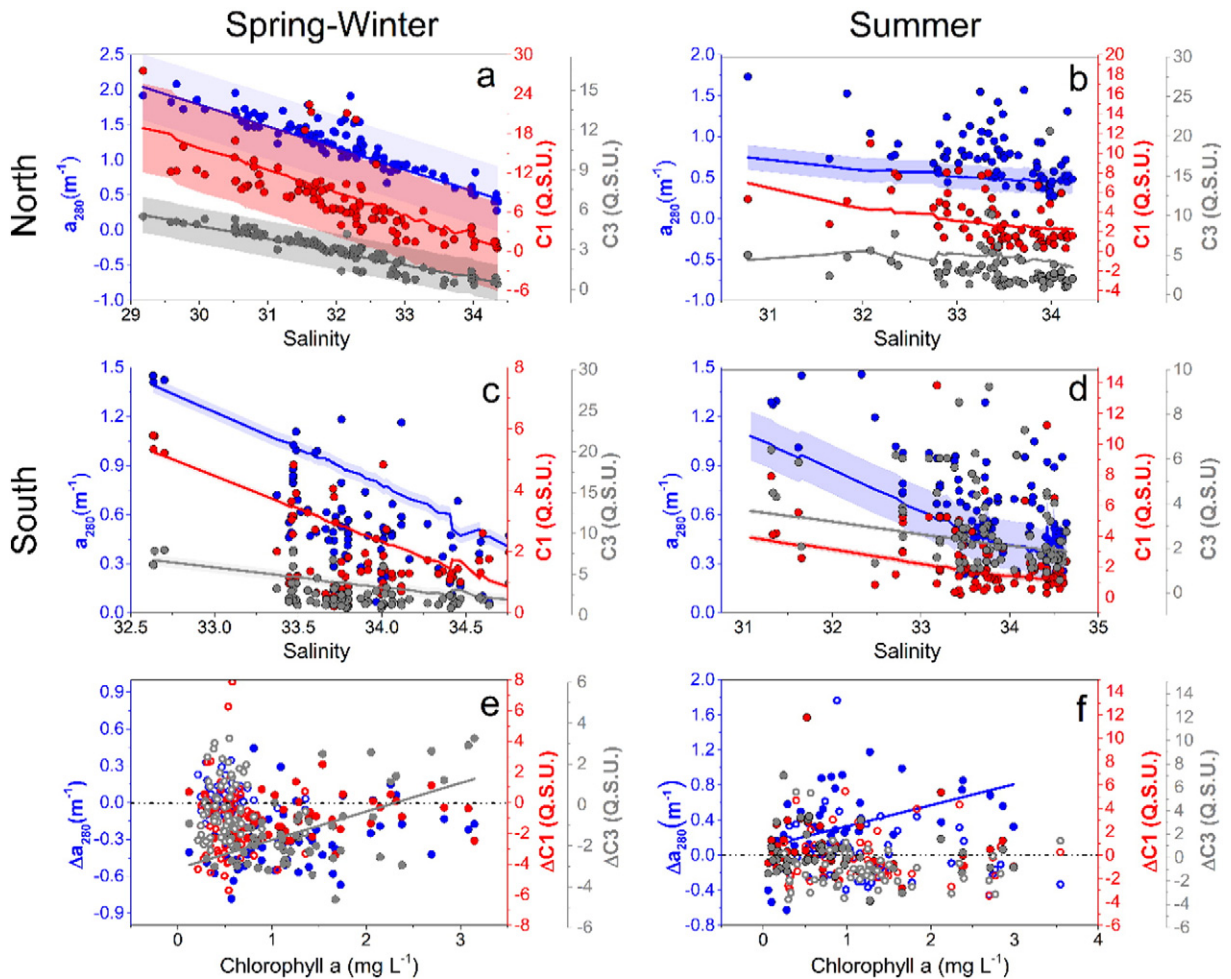


Fig. 9. Correlation between salinity (a–d) and chlorophyll *a* (e–f) with CDOM in the Taiwan Strait. Model estimated conservative mixing line of a_{280} (blue), Components 1 (red) and 3 (grey) and their uncertainties (corresponding colored shadows) are shown in spring-and-winter (a and c) and summer (b and d) of the northern and southern Taiwan Strait. Blue, red and grey dots denote the a_{280} , Components 1 and 3, as well as their differences between field data and model estimation. The open and solid dots in (e) and (f) indicate the northern and southern Taiwan Strait. The grey line in (e) and blue line in (f) indicate the regression line of $\Delta C3$ and Δa_{280} along the increasing chlorophyll *a* in the southern Taiwan Strait.

fluorescent intensities and DOC concentration during winter (Figs. 5 and 7). While lower CDOM, fluorescent intensities and DOC concentration in the southern Taiwan Strait could be induced by diminishing terrestrial input, the higher $S_{275-295}$ might suggest the general LMW and relatively degraded characteristics of CDOM (Fichot and Benner, 2012; Guo et al., 2014, 2011; Helms et al., 2008), which strongly supported the model outcome.

During summer, the CDOM mixing behavior did not present any contrasting geographical difference between the northern and southern Taiwan Strait as was seen in winter (Fig. 9). This was consistent with the coherent hydrological regime throughout the summer Taiwan Strait, which was dominated by the northward flowing SCS seawater and Kuroshio Current with obvious upwelling waters and river plumes (Fig. 3; Hu et al., 2010; Naik and Chen, 2008).

4.2.2. Seasonal variations

Not only geographic variations but also seasonal variations of CDOM mixing behaviors were observed in the Taiwan Strait between spring-and-winter and summer. Nearly 50% removal of CDOM and 30–55% removal of fluorescent components were observed in the southern Taiwan Strait during winter with higher removal rates of protein-like C3 and C1 than humic-like C2, suggesting the more labile characteristics of proteins (Fig. 9b and d; Table 2). This was consistent with previous observations in the estuaries along the western Taiwan Strait coast and other areas showing that protein-like components are susceptible to microbial decomposition and photo-degradation (Fellman et al., 2010; Guo et al., 2011, 2014). Simultaneously, a positive correlation between $\Delta C3$ and chlorophyll *a* concentration was further indicated by the mixing model, which supported the marine algal production of protein-like C3 (Fig. 9e). Considering the in situ contribution of primary production to protein-like C3, its actual removal rate from the southern Taiwan Strait during winter could be more significant than the apparent removal rate indicated by the mixing model.

On average, bulk CDOM, indicated by a_{280} , and riverine fluorescent C1 received a 13% addition as revealed by the three end-member mixing model while terrestrial fluorescent C2 and freshly produced marine fluorescent C3 remained quite conservative with negligible (1–3%) removal compared to the model uncertainty in the whole Taiwan Strait during summer (Table 2). The addition of bulk CDOM to the Taiwan Strait in summer was likely to have been contributed by primary production as suggested by the significant positive correlation between Δa_{280} and the chlorophyll *a* concentration in the southern Taiwan Strait, although such a correlation was not found in the northern Taiwan Strait (Fig. 9f). Widespread upwelling systems bring nutrient abundant SCSsubW into the Taiwan Strait and thus stimulate phytoplankton growth (Chen, 2008; Hong et al., 2011b). Owing to the intensive anthropogenic impacts in southeastern China, the coastal rivers also discharge an increasing nutrient load into the northern SCS and the Taiwan Strait (Han et al., 2012; Yan et al., 2012). The anthropogenic nutrient input could further enhance the primary production in the study area. Previous investigations have revealed relatively abundant DOM in the Taiwan Strait which are in fresh colloidal form and have potentially high bioavailability (Chen, 2008; Lin, 2013). Even under nutrient depleted conditions, the dissolved organic nutrients (including dissolved organic nitrogen and phosphorus) can still support a significant amount of biomass in the Taiwan Strait (Chen, 2008). However, the autochthonous protein-like C3 did not exhibit a significant correlation with chlorophyll *a* concentration (Fig. 9f). Considering the higher water temperature and more intensive solar radiation in summer, the microbial decomposition and photo-degradation of CDOM was expected to be strongest at this time of year. The freshly produced protein-like substances could undergo more intensive decomposition than bulk CDOM owing to its labile characteristic and thus obscure its relationship with primary production (Fellman et al., 2010; Guo et al., 2014, 2011).

Another source of additional CDOM could be the input of riverine autochthonous CDOM since a 13% addition of riverine protein-like C1 was

also revealed (Table 2). Although the riverine input had been included as the end-member of the DW in the mixing model estimation, the various major river sources in the Taiwan Strait with different human impacts and basin-wide hydrographic settings, including the Minjiang, Jiulong and Pearl Rivers, would challenge the identification of the riverine end-member and enlarge the model uncertainty more than expected (He et al., 2010; Yan et al., 2012). Guo et al. (2014) also reveal the variable CDOM compositions in southeastern Chinese rivers which show a significantly different CDOM fraction in the bulk DOM pool than do other major world rivers. On the other hand, there are abundant small ungauged coastal rivers along the west coast of the Taiwan Strait besides the aforementioned major rivers. Although no data is currently available, the contribution from these small rivers cannot be ignored.

Based on the contrasting seasonal and geographical variation of its CDOM mixing behavior, the Taiwan Strait could act as a significant CDOM sink in the southern part of the Strait during winter while as a moderate CDOM source during summer, likely contributed by the freshwater and marine primary productivity. The CDOM was also mixed conservatively in the northern part of the Taiwan Strait during winter. Although hydrological variation as well as the CDOM sources and reactivity were determined to play a focal role in controlling the distribution and quality of CDOM in the Taiwan Strait, the details of interaction, coupling and biogeochemical feedback among the hydrology, biology and physiochemical processes remain ambiguous and warrant further investigation.

5. Conclusions

The spatio-temporal distribution of bulk CDOM and fluorescent components were examined along with their mixing behavior in the Taiwan Strait during 2012 in spring, summer and winter. The application of EEMs and PARAFAC identified two protein-like fluorescent components (C1 and C3) and one humic-like fluorescent component (C2). Both spatial and seasonal distribution of bulk CDOM and terrestrially derived fluorescent components (C1 and C2) showed significant variations with higher intensity in the Min-Zhe Coastal Current dominated water mass and river plume waters, and with decreases offshore, which were dominated by the SCS seawater and the Kuroshio Current, implying the importance of terrigenous input and hydrological transport and mixing in shaping the CDOM dynamics in the Taiwan Strait. The increasing absorption spectral slope between 275 and 295 nm ($S_{275-295}$) from onshore to offshore and from spring-and-winter to summer further revealed the control of CDOM quality by the hydrological regimes in the Taiwan Strait while bacterial decomposition and photo-degradation of CDOM would further cause the variation of $S_{275-295}$. Based on the hydrological characteristics as revealed in the θ -S diagram, three water mass end-members were determined: the SCSW, SCSsubW and DW (i.e. Min-Zhe Coastal Current during winter and river plume waters during summer), and were further applied in a three end-member mixing model to evaluate the CDOM mixing behavior in the Taiwan Strait. During winter, a conservative mixing of CDOM occurred in the northern Taiwan Strait, while a significant (33–54%) removal of bulk CDOM and individual fluorescent components was observed in the south. Instead, a 13% addition of bulk CDOM and riverine fluorescent C1 was indicated throughout the whole Taiwan Strait during summer. The significant correlation between bulk CDOM addition and chlorophyll *a* concentration in the southern Taiwan Strait suggested the contribution of additional CDOM from the primary production in the summer Taiwan Strait, although riverine input from ungauged small coastal rivers could be another potential source.

Acknowledgements

The authors wish to thank Liangshi Lin, Feiyun Pan, Shangshang Bi, Wei Qian for sample collection and data analysis, and two anonymous reviewers for their constructive comments. We are also grateful to the

captain and crew of the R/V *Yanping II* for their sampling assistance on board. This work was supported in part by the National Basic Research Program (973 Program) sponsored by the Ministry of Science and Technology (2014CB953700 and 2014CB953702), the National Natural Science Foundation of China (41276063 and 40906040), the Natural Science Foundation of Fujian Province of China (2015Y00040), the Public Science and Technology Research Fund of the State Oceanic Administration of China (201505034), the Fundamental Research Funds for the Central Universities of China and the Scientific Research Foundation for Returned Overseas Chinese Scholars, the Ministry of Education China. Professor John Hodgkiss of The University of Hong Kong is thanked for his help with English.

Appendix A. Supplementary data

Supplementary data to this article can be found online at <http://dx.doi.org/10.1016/j.marchem.2016.11.001>.

References

- Barbeau, K., Rue, E.L., Bruland, K.W., Butler, A., 2001. Photochemical cycling of iron in the surface ocean mediated by microbial iron(III)-binding ligands. *Nature* 413, 409–413.
- Bergquist, B.A., Wu, J., Boyle, E.A., 2007. Variability in oceanic dissolved iron is dominated by the colloidal fraction. *Geochim. Cosmochim. Acta* 71, 2960–2974.
- Bianchi, T.S., Garcia-Tigreros, F., Yvon-Lewis, S.A., Shields, M., Mills, H.J., Butman, D., Osburn, C., Raymond, P.A., Shank, G.C., DiMarco, S.F., Walker, N., Reese, B.K., Mullins-Perry, R., Quigg, A., Aiken, G.R., Grossman, E.L., 2013. Enhanced transfer of terrestrially derived carbon to the atmosphere in a flooding event. *Geophys. Res. Lett.* 40, 116–122.
- Blough, N.V., Del Vecchio, R., 2002. Chromophoric DOM in the coastal environment. In: Hansell, D.A., Carlson, C.A. (Eds.), *Biogeochemistry of Marine Dissolved Organic Matter*. Academic Press, pp. 509–546.
- Cai, Y., Guo, L., Douglas, T.A., 2008. Temporal variations in organic carbon species and fluxes from the Chena River, Alaska. *Limnol. Oceanogr.* 53, 1408–1419.
- Cai, Y., Guo, L., Wang, X., Lohrenz, S.E., Mojzsis, A.K., 2013. Effects of tropical cyclones on river chemistry: a case study of the lower Pearl River during Hurricanes Gustav and Ike. *Estuar. Coast. Shelf Sci.* 129, 180–188.
- Chen, C.-T.A., 2008. Distributions of nutrients in the East China Sea and the South China Sea connection. *J. Oceanogr.* 64, 737–751.
- Chen, C.-T.A., Hsing, L.-Y., Liu, C.-L., Wang, S.-L., 2004. Degree of nutrient consumption of upwelled water in the Taiwan Strait based on dissolved organic phosphorus or nitrogen. *Mar. Chem.* 87, 73–86.
- Coble, P.G., 2007. Marine optical biogeochemistry: the chemistry of ocean color. *Chem. Rev.* 107, 402–418.
- Cory, R.M., McKnight, D.M., 2005. Fluorescence spectroscopy reveals ubiquitous presence of oxidized and reduced quinones in dissolved organic matter. *Environ. Sci. Technol.* 39, 8142–8149.
- Dai, M., Meng, F., Tang, T., Kao, S.-J., Lin, J., Chen, J., Huang, J.-C., Tian, J., Gan, J., Yang, S., 2009. Excess total organic carbon in the intermediate water of the South China Sea and its export to the North Pacific. *Geochem. Geophys. Geosyst.* 10, Q12002. [10.1029/2009GC002752](https://doi.org/10.1029/2009GC002752).
- Del Vecchio, R., Blough, N.V., 2004. On the origin of the optical properties of humic substances. *Environ. Sci. Technol.* 38, 3885–3891.
- Du, C., Shang, S., Dong, Q., Hu, C., Wu, J., 2010. Characteristics of chromophoric dissolved organic matter in the nearshore waters of the western Taiwan Strait. *Estuar. Coast. Shelf Sci.* 88, 350–356.
- Dyhrman, S.T., Chappell, P.D., Haley, S.T., Moffett, J.W., Orchard, E.D., Waterbury, J.B., Webb, E. A., 2006. Phosphonate utilization by the globally important marine diazotroph *Trichodesmium*. *Nature* 439, 68–71.
- Fellman, J.B., Spencer, R.G.M., Hernes, P.J., Edwards, R.T., D'Amore, D.V., Hood, E., 2010. The impact of glacier runoff on the biodegradability and biochemical composition of terrigenous dissolved organic matter in near-shore marine ecosystems. *Mar. Chem.* 121, 112–122.
- Fichot, C.G., Benner, R., 2012. The spectral slope coefficient of chromophoric dissolved organic matter ($S_{275-295}$) as a tracer of terrigenous dissolved organic carbon in river-influenced ocean margins. *Limnol. Oceanogr.* 57, 1453–1466.
- Fichot, C.G., Kaiser, K., Hooker, S.B., Amon, R.M.W., Babin, M., Bélanger, S., Walker, S.A., Benner, R., 2013. Pan-Arctic distributions of continental runoff in the Arctic Ocean. *Sci. Report.* 3, 1053.
- Guo, L., Santschi, P.H., 2007. Ultrafiltration and its applications to sampling and characterization of aquatic colloids. In: Wilkinson, K., Lead, J. (Eds.), *Environmental Colloids and Particles*. John Wiley, pp. 159–221.
- Guo, W., Stedmon, C.A., Han, Y., Wu, F., Yu, X., Hu, M., 2007. The conservative and non-conservative behavior of chromophoric dissolved organic matter in Chinese estuarine waters. *Mar. Chem.* 107, 357–366.
- Guo, W., Yang, L., Hong, H., Stedmon, C.A., Wang, F., Xu, J., Xie, Y., 2011. Assessing the dynamics of chromophoric dissolved organic matter in a subtropical estuary using parallel factor analysis. *Mar. Chem.* 124, 125–133.
- Guo, W., Yang, L., Zhai, W., Chen, W., Osburn, C.L., Huang, X., Li, Y., 2014. Runoff-mediated seasonal oscillation in the dynamics of dissolved organic matter in different branches of a large bifurcated estuary—the Changjiang Estuary. *J. Geophys. Res. Biogeosci.* 119, 776–793.
- Han, A., Dai, M., Kao, S.-J., Gan, J., Li, Q., Wang, L., Zhai, W., Wang, L., 2012. Nutrient dynamics and biological consumption in a large continental shelf system under the influence of both a river plume and coastal upwelling. *Limnol. Oceanogr.* 57, 486–502.
- Han, A., Dai, M., Gan, J., Kao, S.-J., Zhao, X.Z., Jan, S., Li, Q., Lin, H., Chen, C.-T.A., Wang, L., Hu, J., Wang, L.F., Gong, F., 2013. Inter-shelf nutrient transport from the East China Sea as a major nutrient source supporting winter primary production on the northeast South China Sea shelf. *Biogeochemistry* 10, 8159–8170.
- Hansell, D.A., Carlson, C.A., 2015. *Biogeochemistry of Marine Dissolved Organic Matter*. 2nd. Elsevier, p. 667.
- Hansell, D.A., Carlson, C.A., Repeta, D., Schlitzer, R., 2009. Dissolved organic matter in the ocean: a controversy stimulates new insights. *Oceanography* 22, 202–211.
- He, B., Dai, M., Zhai, W., Wang, L., Wang, K., Chen, J., Lin, J., Han, A., Xu, Y., 2010. Distribution, degradation and dynamics of dissolved organic carbon and its major compound classes in the Pearl River estuary. *China. Mar. Chem.* 119, 52–64.
- Helmis, J.R., Stubbins, A., Ritchie, J.D., Minor, E.C., Kieber, D.J., Mopper, K., 2008. Absorption spectral slopes and slope ratios as indicators of molecular weight, source, and photobleaching of chromophoric dissolved organic matter. *Limnol. Oceanogr.* 53, 955–969.
- Hong, H., Chai, F., Zhang, C., Huang, B., Jiang, Y., Hu, J., 2011a. An overview of physical and biogeochemical processes and ecosystem dynamics in the Taiwan Strait. *Cont. Shelf Res.* 31, S3–S12.
- Hong, H., Liu, X., Chiang, K.-P., Huang, B., Zhang, C., Hu, J., Li, Y., 2011b. The coupling of temporal and spatial variations of chlorophyll *a* concentration and the East Asian monsoons in the southern Taiwan Strait. *Cont. Shelf Res.* 31, S37–S47.
- Hu, J., Kawamura, H., Li, C., Hong, H., Jiang, Y., 2010. Review on current and seawater volume transport through the Taiwan Strait. *J. Oceanogr.* 66, 591–610.
- Jan, S., Wang, J., Chern, C.-S., Chao, S.-Y., 2002. Seasonal variation of the circulation in the Taiwan Strait. *J. Mar. Syst.* 35, 249–268.
- Jiao, N., Herndl, G.J., Hansell, D.A., Benner, R., Kattner, G., Wilhelm, S.W., Kirchman, D.L., Weinbauer, M.G., Luo, T., Chen, F., Azam, F., 2010. Microbial production of recalcitrant dissolved organic matter: long-term carbon storage in the global ocean. *Nat. Rev. Microbiol.* 8, 593–599.
- Jørgensen, L., Stedmon, C.A., Kragh, T., Markager, S., Middelboe, M., Søndergaard, M., 2011. Global trends in the fluorescence characteristics and distribution of marine dissolved organic matter. *Mar. Chem.* 126, 139–148.
- Kowalczyk, P., Cooper, W.J., Durako, M.J., Kahn, A.E., Gonsior, M., Young, H., 2010. Characterization of dissolved organic matter fluorescence in the South Atlantic Bight with use of PARAFAC model: relationships between fluorescence and its components, absorption coefficients and organic carbon concentrations. *Mar. Chem.* 118, 22–36.
- Li, M., Xu, K., Watanabe, M., Chen, Z., 2007. Long-term variations in dissolved silicate, nitrogen, and phosphorus flux from the Yangtze River into the East China Sea and impacts on estuarine ecosystem. *Estuar. Coast. Shelf Sci.* 71, 3–12.
- Lin, L., 2013. *Biogeochemical Behavior of Colloidal Organic Phosphorus in the Jiulong River Estuary and Taiwan Strait*. Xiamen University, Master Thesis.
- Liu, K.-K., Chao, S.-Y., Shaw, P.-T., Gong, G.-C., Chen, C.-T.A., Tang, T.Y., 2002. Monsoon-forced chlorophyll distribution and primary production in the South China Sea: observations and a numerical study. *Deep-Sea Res. I Oceanogr. Res. Pap.* 49, 1387–1412.
- Murphy, K.R., Ruiz, G.M., Dunsmuir, W.T.M., Waite, T.D., 2006. Optimized parameters for fluorescence-based verification of ballast water exchange by ships. *Environ. Sci. Technol.* 40, 2357–2362.
- Naik, H., Chen, C.-T.A., 2008. Biogeochemical cycling in the Taiwan Strait. *Estuar. Coast. Shelf Sci.* 78, 603–612.
- Nelson, N.B., Siegel, D.A., 2013. The global distribution and dynamics of chromophoric dissolved organic matter. *Annu. Rev. Mar. Sci.* 5, 447–476.
- Nelson, N.B., Siegel, D.A., Carlson, C.A., Swan, C.M., 2010. Tracing global biogeochemical cycles and meridional overturning circulation using chromophoric dissolved organic matter. *Geophys. Res. Lett.* 37, L03610. [http://dx.doi.org/10.1029/2009GL042325](https://doi.org/10.1029/2009GL042325).
- Rosón, G., Álvarez-Salgado, X., Pérez, F., 1997. A non-stationary box model to determine residual fluxes in a partially mixed estuary, based on both thermohaline properties: application to the Ria de Arousa (NW Spain). *Estuar. Coast. Shelf Sci.* 44, 249–262.
- Stedmon, C.A., Bro, R., 2008. Characterizing dissolved organic matter fluorescence with parallel factor analysis: a tutorial. *Limnol. Oceanogr. Methods* 6, 572–579.
- Stedmon, C.A., Markager, S., 2005. Tracing the production and degradation of autochthonous fractions of dissolved organic matter using fluorescence analysis. *Limnol. Oceanogr.* 50, 1415–1426.
- Stedmon, C.A., Markager, S., Kaas, H., 2000. Optical properties and signatures of chromophoric dissolved organic matter (CDOM) in Danish coastal waters. *Estuar. Coast. Shelf Sci.* 51, 267–278.
- Stedmon, C.A., Markager, S., Bro, R., 2003. Tracing dissolved organic matter in aquatic environments using a new approach to fluorescence spectroscopy. *Mar. Chem.* 82, 239–254.
- Twardowski, M.S., Boss, E., Sullivan, J.M., Donaghay, P.L., 2004. Modeling the spectral shape of absorption by chromophoric dissolved organic matter. *Mar. Chem.* 89, 69–88.
- Walker, S.A., Amon, R.M.W., Stedmon, C.A., Duan, S., Louchouart, P., 2009. The use of PARAFAC modeling to trace terrestrial dissolved organic matter and fingerprint water masses in coastal Canadian Arctic surface waters. *J. Geophys. Res. Biogeosci.* 114, G00F06. [10.1029/2009JG000990](https://doi.org/10.1029/2009JG000990).
- Wang, J., Hong, H., Jiang, Y., Chai, F., Yan, X.-H., 2013. Summer nitrogenous nutrient transport and its fate in the Taiwan Strait: a coupled physical-biological modeling approach. *J. Geophys. Res. Ocean.* 118, 4184–4200.
- Wetz, M.S., Wheeler, P.A., 2007. Release of dissolved organic matter by coastal diatoms. *Limnol. Oceanogr.* 52, 798–807.

- Wu, C.-R., Chao, S.-Y., Hsu, C., 2007. Transient, seasonal and interannual variability of the Taiwan Strait current. *J. Oceanogr.* 63, 821–833.
- Xue, P., Chen, C., Ding, P., Beardsley, R.C., Lin, H., Ge, J., Kong, Y., 2009. Saltwater intrusion into the Changjiang River: a model-guided mechanism study. *J. Geophys. Res.* 114, C02006. <http://dx.doi.org/10.1029/2008JC004831>.
- Yamashita, Y., Jaffe, R., 2008. Assessing the dynamics of dissolved organic matter (DOM) in coastal environments by excitation emission matrix fluorescence and parallel factor analysis (EEM-PARAFAC). *Limnol. Oceanogr.* 53, 1900–1908.
- Yamashita, Y., Nosaka, Y., Suzuki, K., Ogawa, H., Takahashi, K., Saito, H., 2013. Photobleaching as a factor controlling spectral characteristics of chromophoric dissolved organic matter in open ocean. *Biogeosciences* 10, 7207–7217.
- Yan, X., Zhai, W., Hong, H., Li, Y., Guo, W., Huang, X., 2012. Distribution, fluxes and decadal changes of nutrients in the Jiulong River Estuary, Southwest Taiwan Strait. *Chinese Sci. Bull.* 57, 2307–2318.
- Yang, L., Hong, H., Guo, W., Chen, C.-T.A., Pan, P.-I., Feng, C.-C., 2012. Absorption and fluorescence of dissolved organic matter in submarine hydrothermal vents off NE Taiwan. *Mar. Chem.* 128–129, 64–71.
- Yang, L., Hong, H., Chen, C.-T.A., Guo, W., Huang, T.-H., 2013. Chromophoric dissolved organic matter in the estuaries of populated and mountainous Taiwan. *Mar. Chem.* 157, 12–23.
- Zhang, W., Hong, H., Yan, X., 2013. Typhoons enhancing northward transport through the Taiwan Strait. *Cont. Shelf Res.* 56, 13–25.